Imaging pH, metabolism and hypoxia using hyperpolarized ^{13}C-MRI and [^{18}F]FMISO-PET to assess metabolic connectivity and heterogeneity of the tumor microenvironment in glioblastoma *(250 characters, currently: 180)*

Martin Grashei[1], Carolin Kitzberger[2], Jason G. Skinner[1], Sandra Sühnel[1], Geoffrey J. Topping[1], Elisabeth Bliemsrieder[1], Christian Hundshammer[1], Katja Steiger[3], Rainer Glass[4], Wolfgang Weber[1], Christine Spitzweg[2], Franz Schilling[1]

[1]*Department of Nuclear Medicine, Klinikum rechts der Isar, School of Medicine, Technical University of Munich, Munich, Germany*

[2]*Medizinische Klinik und Poliklinik IV-Campus Großhadern, University Hospital of Munich, Ludwig-Maximilians-University Munich, Munich, Germany*

[3]Institute *of Pathology, School of Medicine, Technical University of Munich, Munich, Germany*

[4]*Neurosurgical Research University Clinics, Ludwig-Maximilians-University Munich, Munich, Germany*

Labels: 1. Hyperpolarized MR (non-Gas), 2. Multimodal, 3. Cancer

Keywords: Hyperpolarized ^{13}C-MRSI, Zymonic Acid, pH, Pyruvate, Glioblastoma, [^{18}F]FMISO, PET, Multimodal Imaging

Introduction *(600 characters, includes space characters, currently: 573)*

Glioblastoma (GBM) is a highly malignant and heterogeneous tumor of the central nervous system. Despite a large variety of existing treatment approaches[1], prognosis and outcome are still devastating. However, therapy efficacy often depends on the tumor microenvironment such as extracellular pH and oxygenation and is often driven by tumor metabolism. Here, we studied GBM by multimodal imaging of pH[2,3], pyruvate-lactate conversion and hypoxia using hyperpolarized (HP) ^{13}C-MRI and ^{18}F-PET to investigate links between hypoxia, pH and lactate production in these tumors.

Methods *(800 characters, includes space characters, currently: 801)*

Model: 10 CD-1-nu/nu mice injected subcutaneously with $1 \cdot 10^6$ patient-derived GBM cells undergoing the protocol in Fig. 1a.

HP: 27 mg [1,5-$^{13}C_2$,3,6,6,6-D_4]zymonic acid and 25 mg ^{13}C-urea were polarized by DNP[3] and dissolved in 80 mM TRIS and D_2O. 25 mg [1-^{13}C]pyruvate was polarized and dissolved in 80 mM TRIS and H_2O.

HP MR(S)I: pH-imaging at 7T used FIDCSI with FA 15°, resolution 2x2x5 mm³, BW 3201 Hz, 256 points. Metabolic imaging used bSSFP[4] with $FA_{P/L}$ = 4/90°, resolution (1.75 mm)³, 1.05 s per frame.

PET-Imaging: Mice were imaged with voxel size (0.8 mm)³ 3 hours after injecting 10-15 MBq [^{18}F]Fluoromisonidazole ([^{18}F]FMISO).

Data Processing: pH maps were calculated in MATLAB[2]. Metabolism was quantified by AUC-ratios[5].

Histology: Tumors (FFPE) were stained for carbonic anhydrase 9 (CAIX).

Results/Discussion *(1000 characters, includes space characters, currently: 997)*

Tumor pH-maps (Fig. 1b) reveal pH heterogeneity with acidified hotspots as low as pH = (7.17±0.11, n = 10) and light overall acidification pH = (7.34±0.02, n = 10). Imaging of pyruvate (Fig. 1c) and lactate (Fig. 1d) shows strong, heterogeneous lactate production quantified by AUC = (1.14±0.17, n = 8). No correlation between acidification and pyruvate-lactate metabolism is observed (Fig. 2b). [^{18}F]FMISO-PET indicates increased tumor uptake with SUV_{mean} = (0.49±0.05, n = 7) relative to muscle tissue (SUV_{muscle} = 0.11±0.01, n = 7) (Fig. 2a), correlating strongly with lactate production (Fig. 2c). Histological staining shows strong expression of CAIX (Fig. 2d).
These results suggest that this tumor model uses anaerobic glycolysis to overcome hypoxia. Buffer capacity appears sufficient such that produced lactate only mildly acidifies the extracellular tumor microenvironment, whereas under normoxic conditions, overexpression of CAIX might lead to stronger extracellular acidification[6].

Conclusion *(450 characters, includes space characters, currently: 432)*

We demonstrated a multimodal imaging characterization of a patient-derived GBM model in mice regarding pH, metabolic pyruvate-to-lactate conversion, and hypoxia. Observed hypoxia occurred together with increased lactate-production and mild acidification. Therefore, the tumor microenvironment can be assessed with the described imaging modalities, suggesting their use as predictive imaging biomarkers in the context of GBM therapy.

Acknowledgements

We acknowledge help from Sybille Reder, Markus Mittelhäuser and Hannes Rolbieski for help with PET-Acquisitions, Michael Herz for PET-Tracer Synthesis and Marion Mielke, Olga Seelbach und Tanja Groll from pathology department (CeP) for help with histology. Further, we acknowledge support from the Deutsche Forschungsgemeinschaft (DFG, German Research Foundation – 391523415, SFB 824).

References

1. Anjum K, Shagufta B I, Abbas S Q, et al. Current status and future therapeutic perspectives of glioblastoma multiforme (GBM) therapy: A review. Biomed Pharmacother 2017; 92:681-689

2. Duewel S, Hundshammer C, Gersch M, et al. Imaging of pH in vivo using hyperpolarized ^{13}C-labelled zymonic acid. Nature Commun 8, 15126 (2017).

3. Hundshammer C, Duewel S, Koecher S, et al. Deuteration of Hyperpolarized ^{13}C-Labeled Zymonic Acid Enables Sensitivity-Enhanced Dynamic MRI of pH. Chemphyschem. 2017; 18(18): 2422-2425.

4. Skinner J G, Topping G J, Heid I, et al. Fast 3D hyperpolarized 13C metabolic MRI at 7T using spectrally selective bSSFP. Digital Poster at ISMRM2020 International Conference 2020.

5. Hill D K, Orton M R, Mariotti E, et al. Model Free Approach to Kinetic Analysis of Real-Time Hyperpolarized 13C Magnetic Resonance Spectroscopy Data. PloS ONE 2013; 8(9): e71996

6. Lee S-H, Griffiths J R, How and Why are Cancers Acidic? Carbonic Anhydrase IX and the Homeostatic Control of Tumour Extracellular pH. Cancers 2020, 12, 1616

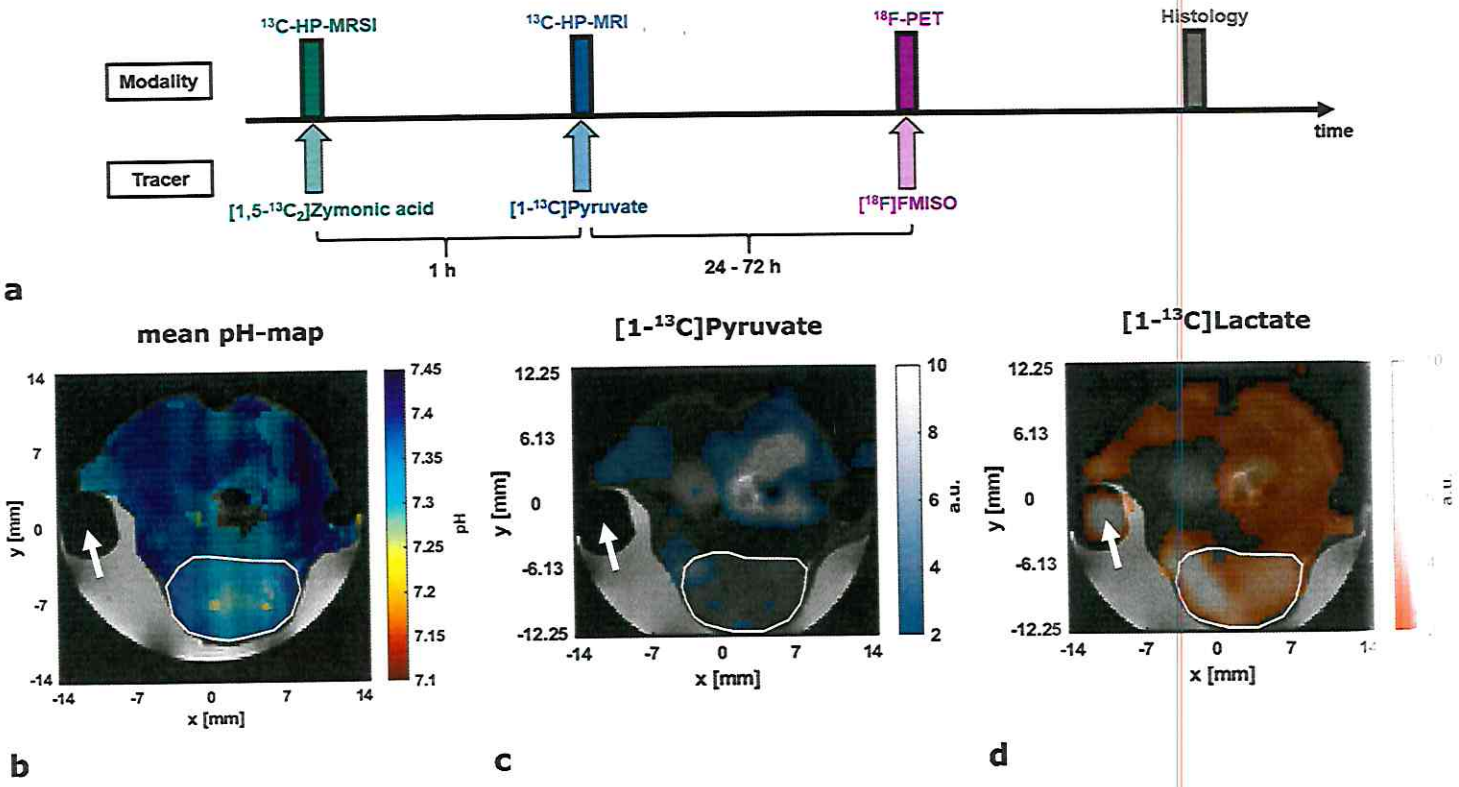

Figure 1: Study Protocol and hyperpolarized ^{13}C-MR(S)I

(figure caption 600 characters incl. space characters, currently: 602)

a: Imaging study protocol showing the temporal sequence and spacing of the applied modalities and injected tracers.

b: Mean pH map weighted by the signal intensity of each compartment in the corresponding voxel overlaid with anatomical image shows mildly acidified tumor regions. Tumor (white ROI) and a [1-^{13}C]lactate-phantom (white arrow) were covered with carbomer gel for shim improvement.

c: Axial [1-^{13}C]pyruvate intensity image overlaid with an anatomical image.

d: Axial [1-^{13}C]lactate intensity image overlaid with an anatomical image shows high lactate production within the tumor (white ROI).

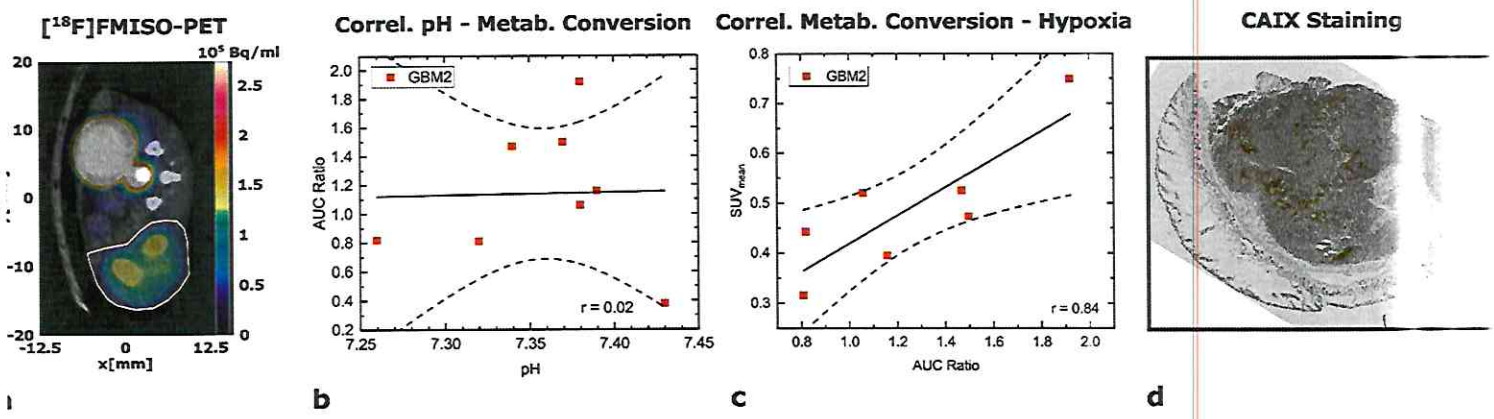

Figure 2: [^{18}F]FMISO-PET, Correlation Plots and Histology

(figure caption 600 characters incl. space characters, currently: 552)

a: Axial image of [^{18}F]FMISO-uptake overlaid with CT. Tumors (white ROI) show increased and heterogeneous uptake compared to healthy tissue (spine muscle).

b: Correlation plot of tumor mean pH with mean pyruvate-lactate AUC ratio. Linear regression shows no correlation (r = 0.02).

c: Correlation plot of tumor metabolic conversion rate AUC ratio and SUV_{mean} for [^{18}F]FMISO. Linear regression shows strong correlation (r = 0.84).

d: Immunohistochemical staining for CAIX. Tissue was sliced according to ^{13}C-MR(S)I. Brown areas indicate positive staining.